FORWARD CONTROL OF AN ELECTROMAGNETIC ACTUATOR USING AN EXPONENTIAL APPROACH

Sarah K. Lami[1], Fawaz F. Al-Bakri[2], Hasan H. Ali[3], Salwan Obaid Waheed Khafaji[4][0000-0001-5144-6895]*
[1]Al-Furat Al-Awsat Technical University (ATU); Technical Institute of Babylon, Iraq
[2]University of Babylon; College of Engineering, Department of Biomedical Engineering, Babylon Iraq
[3]Directorate of Studies, Planning, and, Follow-up; Ministry of Higher Education and Scientific Research, Baghdad Iraq
[4]University of Babylon, College of Engineering, Mechanical Engineering Department, Babylon, Iraq
Email: eng.salwan.obaid@uobabylon.edu.iq

Abstract – An electromagnetic actuator (EMA) represents a heartening approach to take the place of an imitative mechanical actuator system in plenty of workable applications. However, it is unlikely to be functional without achieving a successful execution by designing an active positioning-controller which can stabilize the system rapidly. In this work, a new analytical algorithm for the electromagnetic actuator (EMA) system has been developed. The proposed algorithm aims to generate well-suited reference position, velocity, coil current, and coil voltage profiles that rely on the initial and final states. Firstly, the reference position and velocity are shaped by a series of exponential functions with time as the independent variable. Then, initial and steady-state position, velocity, and acceleration conditions are automatically satisfied to ensure the required reference coil current and voltage. Eventually, extensive initial actuator position dispersions are considered to perform the presented approach using the Monte-Carlo simulation method. The demonstrated results show that the suggested algorithm strategy can greatly stabilize the electromagnetic actuator with a fast response and less overshoot in the presence of wide initial position dispersions.

Keywords: Electromagnetic Actuator, Forward Control, Analytical Approach, Monte Carlo Simulation.

1. Introduction

Electromagnetic actuators that use electromagnetic forces are widely used in industrial applications such as valve actuators in heating systems, internal combustion engines, and the airplane industry. The use of electromagnetic actuators usually requires an accurate control of their motion. Various control strategies have been used to control the motion of electromagnetic actuators. A linear parameter-varying (LPV) technique was developed and a robust controller was designed in [1-2] for the motion control of a nonlinear electromagnetic actuator. A two-degree-of-freedom electromagnetic actuator with a Halbach array structure was studied in [3]. The results showed that the of the proposed system's magnetic field, force coefficients, and torque were larger than those of traditional systems. A model predictive control and a proportional-integral controller of the position of an electromagnetic actuator were investigated in [4]. In [5-7] a sliding mode control method was implemented to control the motion of a nonlinear electromagnetic actuator. In [8], an H-infinity control strategy was used to control the position of an electromagnetic actuator. A nonlinear control law was implemented in [9] taking into account the magnetic phenomenon. In [10], PID and LQR controllers are utilized to investigate the stability of the electromagnetic actuator under load and wave signal variations. The results obtained that the LQR controller is faster and more homogenous than the PID controller. Meanwhile, in [11], A Linear Parameter-Varying (LPV) Approach was used to control the armature velocity to gain low noise and war. The experimental and simulated results illustrated that the proposed controller was simple and successfully able to be used in industrial applications. A fuzzy logic control method was present as well to stabilize the electromagnetic system as in [12]. This nonlinear method effectively controlled the electromagnetic system compared with other linear control methods while considering a range of system uncertainties.

A simple but accurate analytical control strategy in which a single analytical function is used to generate the motion profiles of the system was considered in [13-15]. A motion control system for an actuator is presented in [16-17]. The open loop system was modeled. PID and robust H-infinity controllers were designed. The results showed that the H-infinity controller provides better response while satisfying the robustness requirements.

This work focuses on stabilizing the electromagnetic actuator. The proposed approach creates state and input profiles using a series of exponential functions with time as the independent variable. In addition, the system coil voltage is evaluated online based on the initial actuator position. In such a way, this presented approach is adaptable in the presence of initial position variations, and might significantly considered as an online approach scheme.

2. System Models

The dynamics of a full state-space representation (SSR) of the electromagnetic actuator model can be obtained by the following ordinary differential equations [5].

$$\begin{aligned} \dot{x}_1 &= x_2 \\ \dot{x}_2 &= \frac{1}{m}\left(\frac{1}{2}x_3^2\mu(x_1) + F_{ext}(x_1, x_2)\right) \\ \dot{x}_3 &= \frac{1}{L(x_1)}\left(u - Rx_3 + x_2x_3\mu(x_1)\right) \end{aligned} \tag{1}$$

where F_{ext} is the external force which can be identified as the summation of the friction (λx_2) and spring forces (Kx_1) as shown in Eq. (2).

$$F_{\text{ext}} = -\lambda x_2 - Kx_1 \tag{2}$$

The magnetic permeability $\mu(x_1)$ and magnetic inductance $L(x_1)$ are inversely proportional to the actuator position as shown in Eqs. (3) and (4), respectively.

$$\mu(x_1) = N^2 \frac{\rho_x}{(\rho_x x_1 + \rho_0)^2} \tag{3}$$

$$L(x_1) = \frac{N^2}{(\rho_x x_1 + \rho_0)} \tag{4}$$

where R, N, ρ_x, and ρ_0, λ are coil resistance, coil winding, airgap reluctance, magnetic reluctance, and friction coefficient, respectively. Substituting Eqs. (2,3,4) into Eq. (1), we can obtain the EMA in the affine form:

$$\dot{x} = \begin{bmatrix} x_2 \\ \frac{1}{M}\begin{pmatrix} \frac{1}{2}x_3^2\left(N^2\frac{\rho_x}{(\rho_x x_1 + \rho_0)^2}\right) \\ -(\lambda x_2 + Kx_1) \end{pmatrix} \\ -\frac{(\rho_x x_1 + \rho_0)}{N^2}\begin{pmatrix} Rx_3 - \\ x_3x_2\left(N^2\frac{\rho_x}{(\rho_x x_1 + \rho_0)^2}\right) \end{pmatrix} \end{bmatrix} + \begin{bmatrix} 0 \\ 0 \\ \frac{(\rho_x x_1 + \rho_0)}{N^2} \end{bmatrix} u \tag{5}$$

Our EMA system utilizes practical parameters from a real reliable EMA system as listed in Table 1. [7].

Table 1: EMA system parameters

Parameter	Value	Definition
K	120	Spring stiffness (N/m)
λ	5	Friction coefficient (N/m²)
R	0.4	coil resistor (Oms)
N	70	Coil turn
ρ_x	2.8	Airgap reluctance ($H^{-1}m^{-1}$)
ρ_0	630	Magnetic circuit reluctance($H^{-1}m^{-1}$)
M	0.1	Mass (kg)

The EMA can be illustrated as in Fig. (1) [5]. Where M and K are the piston mass the spring constant, respectively.

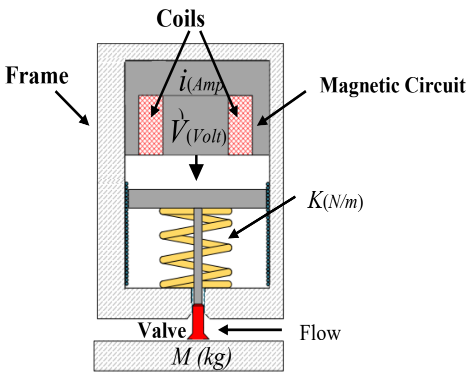

Figure 1: Electromagnetic Actuator Schematic

3. Analytical Reference Approach

A developed analytical control strategy was used in this work to create reference profiles for position, velocity, coil current, and coil voltage that are tailored to the initial and final states. The state space representation model is commonly used to compute a system's eigenvalues, which determine its stability.

To ensure high stability, good damping, and insured tracking performance, either a nonlinear or liner control technique can be introduced. Nevertheless, the forward analytical algorithm is a new technique that controls the EMA position without the need for any feedback control method.

The system employs a series of exponential functions of time to modify the reference profile of the actuator position, velocity, coil current, and coil voltage. The reference actuator position can be obtained as:

$$x_{1\mathrm{ref}} = \sum_{m=1}^{6} C_m \exp(kmt) \tag{6}$$

The system velocity is the time derivative of the actuator position.

where k=10^{-5} and m=1, 2, 3, ...6 are the normalization factor and index, respectively.

$$x_{2\mathrm{ref}} = \sum_{m=1}^{6} mkC_m \exp(kmt) \tag{7}$$

The vehicle acceleration is the time derivative of the diving velocity:

$$\dot{x}_{2\mathrm{ref}} = \sum_{m=1}^{6} k^2 m^2 C_m \exp(kmt) \tag{8}$$

By substituting Eqs. (6), (7), and (8) into Eq. (5) and solving for the reference actuator current (x_3), the reference coil current can be rewritten as:

$$x_{3\mathrm{ref}} = \sqrt{\frac{2\begin{pmatrix} M\left(\sum_{m=1}^{6} m^2k^2C_m \exp(kmt)\right)+ \\ \begin{pmatrix} \lambda\left(\sum_{m=1}^{6} mkC_m \exp(kmt)\right)+ \\ K\left(\sum_{m=1}^{6} C_m \exp(kmt)\right) \end{pmatrix} \end{pmatrix}}{\left(N^2 \dfrac{\rho_x}{\left(\rho_x\left(\sum_{m=1}^{6} C_m \exp(kmt)\right)+\rho_0\right)^2} \right)}} \tag{9}$$

Substituting the reference position [Eq. (6)], reference velocity [Eq. (7)], reference acceleration [Eq. (8)], reference coil current [Eq. (9)], and the time derivative of reference coil current into Eq. (5) and solving for the reference actuator voltage (u), we can get:

$$\begin{aligned} u = {} & R\begin{pmatrix} 2\left(\rho_0+\rho\left(\sum_{m=1}^{6} C_m \exp(kmt)\right)\right)^2 + \left(M\sum_{m=1}^{6} m^2k^2C_m \exp(kmt)\right)+ \\ \left(K\sum_{m=1}^{6} C_m \exp(kmt)\right)/\,N^2\rho \end{pmatrix}^{0.5} + \\ & \frac{\sum_{m=1}^{6} C_m \exp(kmt)\left(4\rho_0+4\rho\sum_{m=1}^{6} C_m \exp(kmt)\right)\begin{bmatrix} \left(\lambda\sum_{m=1}^{6} mkC_m \exp(kmt)\right)+ \\ \left(M\sum_{m=1}^{6} m^2k^2C_m \exp(kmt)\right)+ \\ \left(K\sum_{m=1}^{6} C_m \exp(kmt)\right) \end{bmatrix}}{N^2} + \\ & \frac{\begin{bmatrix} 2\left(\rho_0+\rho\left(\sum_{m=1}^{6} C_m \exp(kmt)\right)\right)^2\left(\lambda\sum_{m=1}^{6} mkC_m \exp(kmt)\right)+\left(M\sum_{m=1}^{6} m^2k^2C_m \exp(kmt)\right) \\ +\left(K\sum_{m=1}^{6} C_m \exp(kmt)\right) \end{bmatrix}}{N^2\rho\begin{bmatrix} \left(\lambda\sum_{m=1}^{6} mkC_m \exp(kmt)\right) \\ +\left(M\sum_{m=1}^{6} m^2k^2C_m \exp(kmt)\right) \end{bmatrix}^{0.5}} \end{aligned} \tag{10}$$

To evaluate the seven function coefficients C_m, it is necessary to have seven boundary conditions. In this case, we applied one pair of actuator position, (x_{1_0}, t_0), velocity (x_{2_0}, t_0), and acceleration ($\dot{x}_{2\_0}$, t_0) at the initial state, one pair of actuator position(x_{1_s},t_s), velocity (x_{2_s},t_s), and acceleration ($\dot{x}_{2\_s}$,t_s). The initial actuator acceleration ($\dot{x}_{2\_s}$) can be evaluated using Eqs. (1), (2), and (3).

Table 2 presents the initial and steady-state conditions for the EMS system.

Table 2: Initial and steady-state conditions for the EMA system

Condition	Value	Definition
t_0	0	Initial time (sec)
x_{2_0}	0	Initial actuator velocity (m/s)
$\dot{x}_{2\_0}$	0	Initial actuator acceleration (m/s^2)
x_{3_0}	4	Initial actuator current (amp)
t_s	0.3	Steady-state time (sec)
x_{1_s}	0.005	Steady-state actuator position (m)
x_{2_s}	0	Steady-state actuator velocity (m/s)
$\dot{x}_{2\_s}$	0	Steady-state acceleration (m/s^2)

The EMA system starts from rest mode and goes into rest mode. As well as the initial coil current has been chosen so that the coil voltage does not exceed in any case the allowable maximum value (V_{max} =200 V) [5]. Finally, the Gaussian elimination method was used to solve the EMA linear system equations with seven variables, allowing for the computation of function coefficients as shown in the following equations:

$$\begin{pmatrix} C_1 = 0.1174 - 6.8x_{1\_0} \\ C_2 = 65.0246x_{1\_0} - 0.846 \\ C_3 = 2.775 - 236.243x_{1\_0} \\ C_4 = 401.605x_{1\_0} - 4.54 \\ C_5 = 3.5572 - 314.568x_{1\_0} \\ C_6 = 91.984x_{1\_0} - 1.06 \end{pmatrix} \quad (11)$$

As we can see from Eq. (11), each coefficient has only one value for any initial actuator position. It is worth mentioning that if the initial actuator position changes, the electromagnetic system will entirely follow a different path to achieve the desired steady-state position.

The main goal of this approach is to end up with a single equation with the reference actuator voltage on the left-hand side and the initial actuator position (x_{1_0}) and the time on the right-hand side as illustrated in Eq. (10). Hence when the electromagnetic system senses its initial actuator position, the forward actuator voltage will be computed analytically without any feedback evaluations.

Figures (1a) - (1d) show the reference actuator position, actuator velocity, coil current, and coil voltage, respectively vs. time, under nominal initial conditions [x_{1_0}=0 and x_{1_0}=0.01] m. As we can see from Figs. (1a) and (1b) that the EMA reaches the steady state position with no overshot while it captures concurrently the rest mode at the steady state time. Figure (1c) shows that the coil current increases gradually until reaching the steady state value (Iss=5.92 amp) then it remains constant to stabilize the EMA in the required time. Even the EMA has a very small steady state voltage value as shown in Fig.(1d), it needs 5.92 amp as a steady state coil current due to the effect of coil resistance.

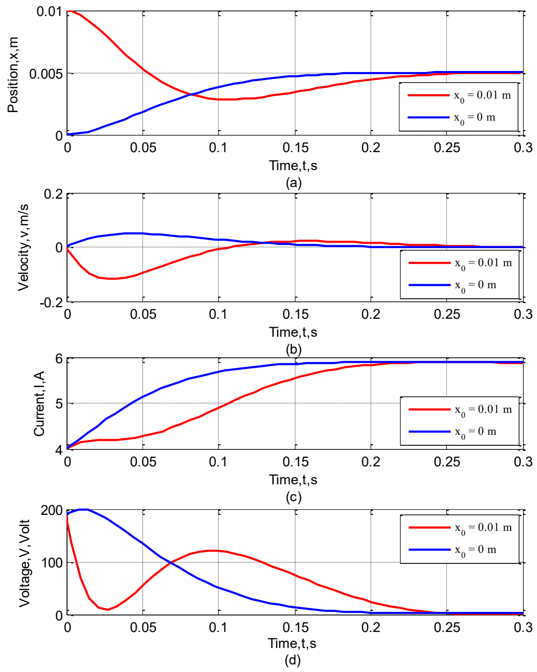

Figure 2: Reference profiles for initial actuator positions $x_{1\text{-}0}$ = 0.01 m and $x_{1\text{-}0}$ = 0 m; (a) actuator position vs. time; (b) actuator velocity vs. time; (c) coil current vs. time; (d) coil voltage vs. time.

4. Nominal Simulation

Any electromagnetic control system aims to quantify and control the actuator position by tracking system reference profiles using a closed-loop control system. This closed-loop system utilizes the notion of feeding the actual output and comparing it with the desired output to reduce the error between them. On the contrary, in this work, the coil voltage control was designed using the forward controller with no feedback loops while achieving the desired actuator position in a short time. For this purpose, the coil voltage was evaluated analytically after attaining the initial and final boundary conditions (Eq.10). Then, the system model was simulated numerically employing the analytical coil voltage (Eq. 5), under the system nominal conditions. Hence, to demonstrate the forward controller, nominal conditions with ($x_{1\text{-}0}$=0 and $x_{1\text{-}0}$=0.01) m are simulated using MATLAB/Ode45 to ensure the performance of the proposed forward algorithm to stabilize the EMA in the required time.

Figures (3-5) and (6-8) present the reference profiles under ($x_{1\text{-}0}$=0 and $x_{1\text{-}0}$=0.01) m, respectively. As is evident from Figs. (3) and (6), the actual actuator positions converge to the reference ones perfectly with -0.8(10^{-10}) m as a maximum calculated error. Figures (4) - (7) and Figs. (5) -(8) show that the actual EMA system satisfies a remarkable tracking of reference velocities with -1.5(10^{-8}) m/s^2 and reference currents with 2(10^{-8}) amp, respectively, as the topmost errors under nominal conditions.

To put it succinctly, the EMA position response using the forward controller has exceedingly improved: the overshoot of the system is mostly non-existent, the system realizes great damping with completely no oscillation, and the settling time has valuably enhanced. Despite that, it is not likely to assuredly execute the presented scheme relying on nominal conditions. For that reason, initial actuator positions between 0 and 0.01 m are randomly simulated using Monte-Carlo Method to ensure the feasibility of the introduced approach.

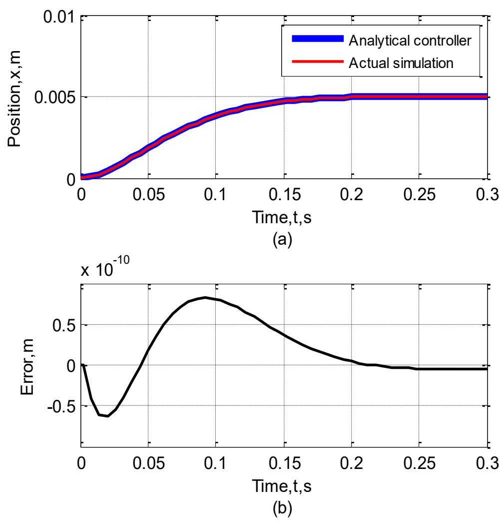

Figure 3: Reference and actual profiles for initial actuator position $x_{1\text{-}0}$ = 0 m; (a) actuator position vs. time; (b) residual actuator position vs. time.

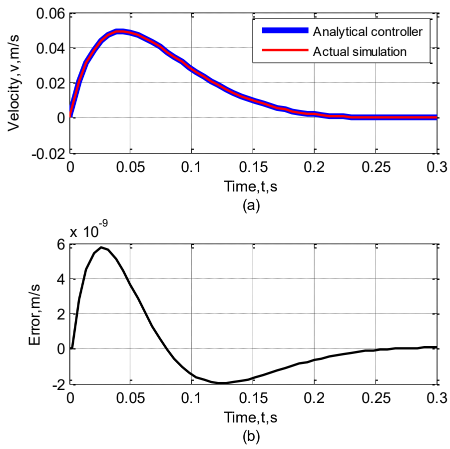

Figure 4: Reference and actual profiles for initial actuator position $x_{1\text{-}0}$ = 0 m; (a) actuator velocity vs. time; (b) residual actuator velocity vs. time.

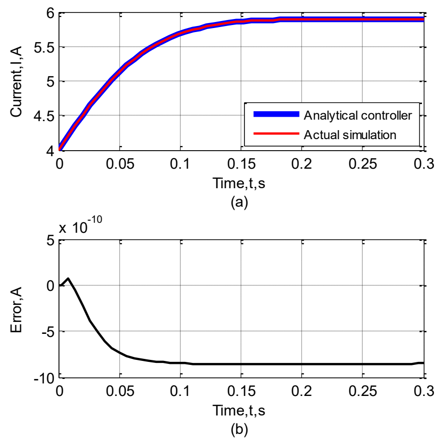

Figure 5: Reference and actual profiles for initial actuator position $x_{1\text{-}0}$ = 0 m; (a) actuator current vs. time; (b) residual actuator current vs. time.

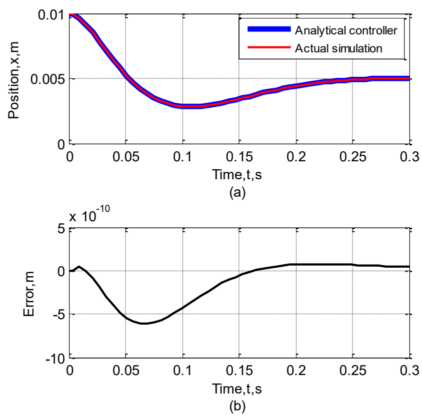

Figure 6: Reference and actual profiles for initial actuator position $x_{1\text{-}0}$ = 0.01 m; (a) actuator position vs. time; (b) residual actuator position vs. time.

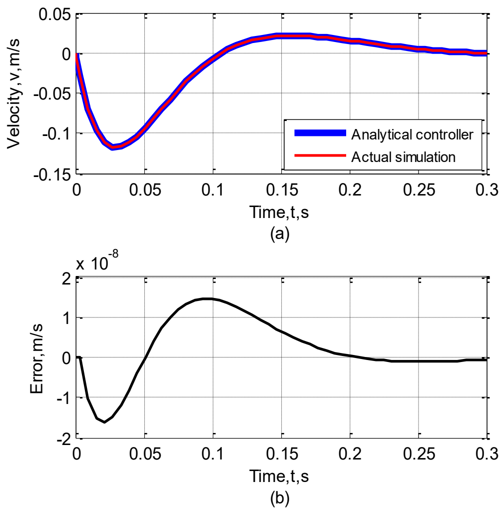

Figure 7 Reference and actual profiles for initial actuator position $x_{1\text{-}0}$ = 0.01 m; (a) actuator velocity vs. time; (b) residual actuator velocity vs. time.

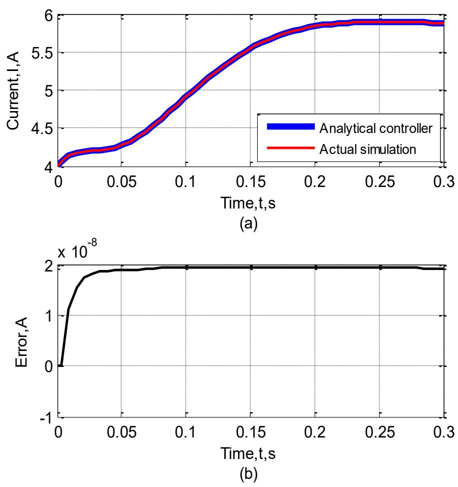

Figure 8 Reference and actual profiles for initial actuator position $x_{1\text{-}0}$ = 0.01 m; (a) actuator current vs. time; (b) residual actuator current vs. time.

While comparing current actuator position with prior studies [5], the proposed analytical algorithm features the ability of stabilizing the (EMA) rapidly without exceeding the voltage constraints. Figures (3,4, and 5) show that the new method ensures a better settling time up to (0.2) sec than the previous time (0.35) sec under the same parametric and initial conditions.

5. Off-Nominal Simulation

A Monte Carlo method is a pattern utilized to anticipate the probability of a diversity of results when the potential for random variables exists. It needs appointing various values to attain several results and after that collecting the results to gain a rough calculation [18-21].

In this work, 2000 Monte-Carlo trials were carried out to test the effectiveness and precision of the presented forward algorithm involving extensive initial actuator position dispersions. The range of random initial actuator position deviations has been selected between 0 and 0.01 m.

Figures (9a) - (9d) present the off-nominal actuator position, actuator velocity, coil current, and coil voltage histories, respectively. As we can see from Figs. (9a) - (9c), the actual profiles tracked greatly the reference ones while EMA can capture the steady-state position in the required time without involving any feedback command. Figure (9d) shows that all the coil voltage profiles do not exceed the allowable voltage (V_{max} =200 Volt) in all of the dispersed tests. The statistical errors for the final actuator position, velocity, current, and voltage are summarized in Table 3. As noted in Table 3, the minimum and maximum errors are very small as well as the mean and standard deviation values are nearly zero. Hence, Monte-Carlo simulation runs are implemented to further perform the effectuality and reliability of the proposed scheme.

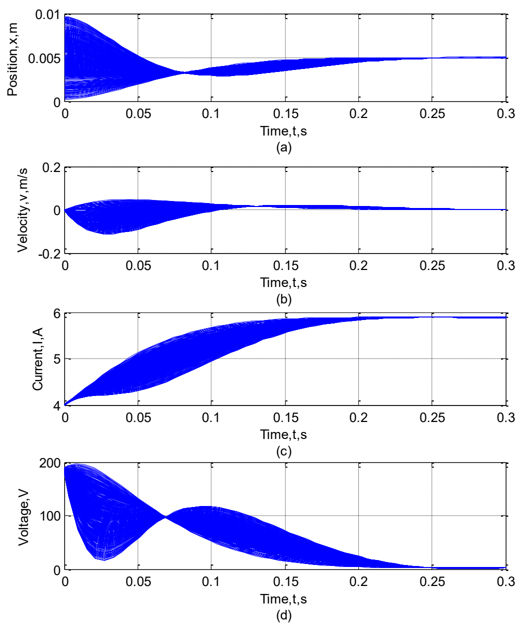

Figure 9 Actual simulation profiles for 2000 Monte-Carlo trials; (a) actuator position vs. time; (a); (b) actuator velocity vs. time; (c) coil current vs. time; (d) coil voltage vs. time.

Table 3 Statistics for final errors

State error	Mean	Standard deviation	Minimum	Maximum
Actuator Position (m)	1.4(10^{-11})	7.9 (10^{-9})	-1.9 (10^{-7})	8.9 (10^{-8})
Actuator velocity (m/s)	-3.4 (10^{-5})	1.2 (10^{-5})	-6.1 (10^{-5})	-1.4 (10^{-5})
Coil current (A)	1.1 (10^{-4})	3.8 (10^{-5})	4.3 (10^{-5})	2.2 (10^{-4})
Coil voltage (Volt)	0.0084	0.0143	-0.007	0.054

6. Conclusions

The electromagnetic actuator with mechanical and electrical concepts has been studied. This work proposed an improved forward approach for stabilizing the EMA based on solving an exponential function while achieving the initial and final boundary conditions. After the reference actuator position and velocity profiles were shaped, the system of ordinary differential equations was used to handle the reference coil current and voltage based on the current initial actuator position. Nominal and off-nominal initial actuator positions were simulated and the results indicated the forward approach can verify potential performance despite the wide range of initial position dispersions.

In summary, the simulated results illustrated the effectiveness of the proposed analytical controller, in order to stabilize the electromagnetic actuator rapidly. The presented controller can be able to solve instability issues in (0.2) sec while maintaining the coil voltage up to the 200 Volt in all of the dispersed tests.

References

[1] Forrai, A., Ueda, T. and Yumura, T., 2007. Electromagnetic actuator control: A linear parameter-varying (LPV) approach. IEEE Transactions on Industrial Electronics, 54(3), pp.1430-1441.

[2] Sengupta, Anirban, and Dushmanta Kumar Das., 2022. Delay dependent wide area damping controller design for a linear parameter varying (LPV) power system model considering actuator saturation and changing environmental condition, 47 (2), pp. 78.

[3] Yang, F., Zhao, Y., Li, H., Mu, X., Zhang, W., Yue, H. and Liu, R., 2022. Design and Analysis of a 2-DOF Electromagnetic Actuator with an Improved Halbach Array for the Magnetic Suspension Platform. Sensors, 22(3), p.790.

[4] Hasan, M.D.S., El Hafni, A. and Kennel, R., 2017, September. Position control of an electromagnetic actuator using model predictive control. In 2017 IEEE International Symposium on Predictive Control of Electrical Drives and Power Electronics (PRECEDE) (pp. 37-41). IEEE.

[5] Uchida, M., Murata, R., Yabumi, T., Morita, Y. and Kando, H., 2006, October. Sliding mode servo control for electromagnetic engine valve. In 2006 SICE-ICASE International Joint Conference (pp. 3658-3663). IEEE.

[6] Al-Bakri, F.F., Lami, S.K., Ali, H.H. and Khafaji, S.O.W., 2021, September. A Sliding Mode Control of an Electromagnetic Actuator Used in Aircraft Systems. In 2021 5th Annual Systems Modelling Conference (SMC) (pp. 1-5). IEEE.

[7] Wan, Shaoke, Xiaohu Li, Wenjun Su, Junpeng Yuan, and Jun Hong, 2020. Active chatter suppression for milling process with sliding mode control and electromagnetic actuator. Mechanical Systems and Signal Processing. 136. pp. 106528.

[8] Mianzo, L. and Peng, H., 2007. Output Feedback H∞ Preview Control of an Electromechanical Valve Actuator. IEEE Transactions on Control Systems Technology, 15(3), pp.428-437.

[9] Deschaux, F., Gouaisbaut, F. and Ariba, Y., 2018, December. Nonlinear control for an uncertain electromagnetic actuator. In 2018 IEEE Conference on Decision and Control (CDC) (pp. 2316-2321). IEEE.

[10] Yaseen, M.H., 2017. A comparative study of stabilizing control of a planer electromagnetic levitation using PID and LQR controllers. Results in physics, 7, pp.4379-4387.

[11] Forrai, A., Ueda, T. and Yumura, T., 2007. Electromagnetic actuator control: A linear parameter-varying (LPV) approach. IEEE Transactions on Industrial Electronics, 54(3), pp.1430-1441.

[12] Koroishi, E.H., Steffen, V. and Mahfoud, J., 2012. Fuzzy Control of Rotor System Using an Electromagnetic Actuator. In MATEC Web of Conferences (Vol. 1, p. 09003). EDP Sciences.

[13] Al-Bakri, F.F., Khafaji, S.O.W. and Ali, H.H., 2021. A NOVEL ANALYTICAL CONTROL OF A SINGLE ROTARY INVERTED PENDULUM UNDER INITIAL ANGULAR DISPERSIONS. International Journal of Mechatronics and Applied Mechanics, (10), pp.32-42.

[14] Al-Bakri, F.F., Ali, H.H. and Waheed, K.S.O., 2021. A new analytical control strategy for a magnetic suspension system under initial position dispersions. FME Transactions, 49(4), pp.977-987.

[15] Ali, H.H., Al-Bakri, F.F. and Khafaji, S.O.W., 2023. Analytical position control system of a linear hydraulic actuator used in aircraft applications. International Journal of Mechatronics and Applied Mechanics, (13), pp.209-218.

[16] Ali H, Fales R, Manring N (2019) Modeling and control design for an inlet metering valve-controlled pump used to control actuator velocity via H-infinity and two-degrees-of-freedom methods. Journal of Dynamic systems, measurement, and control. 141(11), pp. 111006.

[17] Ali, H.H., Mustafa, A.W. & Al-Bakri, F.F. 2021, A new control design and robustness analysis of a variable speed hydrostatic transmission used to control the velocity of a hydraulic cylinder. Int. J. Dynam. Control 9, pp.1078–1091

[18] Al, B.F.F., Khafaji, S.O.W. and Ali, H.H., 2022. Adaptive model Predictive control for a magnetic suspension system under initial position dispersions and voltage disturbances. FME Transactions, 50(1), pp.211-222.

[19] Al-Bakri, F.F., Khafaji, S.O.W., Ali, H.H. and Muhi, L.N., 2021, January. Adaptive Model Predictive Control for a TORA System under Initial Axial and angular Position Dispersions. In 2021 IEEE 11th Annual Computing and Communication Workshop and Conference (CCWC) (pp. 1294-1299). IEEE.

[20] Laheeb, M., Salwan, K., Fawaz, A.B. and Sarah, L., 2018, January. Online algorithm for controlling a cruise system under uncertainty in design parameters and environmental conditions using Monte-Carlo simulation. In 2018 IEEE 8th Annual Computing and Communication Workshop and Conference (CCWC) (pp. 424-430). IEEE.

[21] Fawaz, A.B., Laheeb, M. and Salwan, K., 2018, January. Online algorithm for controlling an inverted pendulum system under uncertainty in design parameters and initial conditions using Monte-Carlo simulation. In 2018 IEEE 8th Annual Computing and Communication Workshop and Conference (CCWC) (pp. 1-7). IEEE.